Numerical **Weather Prediction**

Forecasting Research
Technical Report No. 255

Cloud Height Determination using GOES Water Vapour and Infrared Window Channel Imagery

by

M A Ringer

October 1998

The Met.Office

Excelling *in weather services*

Forecasting Research
Technical Report No. 255

Cloud Height Determination using GOES Water Vapour and Infrared Window Channel Imagery

by

M A Ringer

October 1998

Meteorological Office
NWP Division
Room 344
London Road
Bracknell
Berkshire
RG12 2SZ
United Kingdom

Please notify us if you change your address or no longer wish to receive these publications.

Tel: 44 (0)1344 856245 Fax: 44 (0)1344 854026 e-mail: jsarmstrong@meto.gov.uk

Cloud Height Determination using GOES Water Vapour and Infrared Window Channel Imagery

Mark Ringer

Satellite Imagery Applications Group
Numerical Weather Prediction Division

maringer@meto.gov.uk

Abstract

A method for determining the height of semi-transparent cirrus cloud using radiance measurements in the infrared window and water vapour spectral regions is applied to the relevant channels of the GOES imaging radiometer. In addition to the satellite observations, the method also involves forward modelling the IR and WV radiances for opaque cloudy and clear scenes. This is achieved using atmospheric profiles from the ARPEGE and ECMWF forecast models together with a version of RTTOV adapted to the GOES channels. This report discusses the quality of the simulated radiances, particularly those for clear sky conditions and presents some examples of the application of the height determination method. Comparisons are made between this technique and another, based on the brightness temperature difference between the IR split-window channels of the GOES instrument.

This study was performed during the period 15th June - 4th September 1998, while the author was a visiting scientist at C.M.S. Lannion, France. The visit was organised within the framework of the Nowcasting Satellite Applications Facility and was funded by EUMETSAT.

1 Introduction

For uniform scenes of opaque clouds, filling the field-of-view, the retrieval of the cloud top pressure is relatively straightforward, as the blackbody emission of opaque clouds in the infrared window approximates well to the radiance measured by the satellite. In such circumstances, the cloud top pressure can be estimated as the level of best agreement between the measured infrared window brightness temperature and the temperature profile from a numerical forecast model. The height assignment of semi-transparent cloud (e.g. cirrus) or sub-pixel cloud (i.e. not filling the field-of-view) is, however, much more difficult, as account needs to taken of the background contribution to the measured radiance. This results in the IR window brightness temperature being an overestimate of the cloud temperature, so that the heights of semi-transparent or sub-pixel cloud determined solely from IR window measurements and a model temperature profile are generally too low.

Various methods, using combinations of satellite radiances measured at different wavelengths, have been suggested for correcting for this background radiation contribution and achieving a more reliable height assignment for such clouds: e.g. Inoue (1985); Menzel *et al.* (1983); Szejwach (1982); Lin and Coakley (1993). In this short study a method using measurements in the IR window and water vapour bands applied to data from the GOES imaging radiometer is investigated. The method makes use of the satellite radiances in combination with atmospheric profiles from both the ARPEGE and ECMWF forecast models.

2 Description of the height assignment technique

The details of the technique, known as 'Water vapour-infrared window intercept method' or the 'Eumetsat method', can be found in Schmetz *et al.* (1993) and Nieman *et al.* (1993). A brief summary is given here. The fundamental assumption of the method is that a linear relationship exists between measurements in two spectral bands observing a single cloud layer. In particular, all pairs of measurements in the water vapour and IR window channels viewing a cloud layer at pressure p_c will lie on straight line, with the variation along this line corresponding to changing cloud amount.

The radiance measurements are used in conjunction with radiative transfer calculations of the top-of-the-atmosphere radiance emanating from opaque clouds at different atmospheric levels. The temperature and humidity profiles for these calculations are obtained from a numerical forecast model. The intersection of the measured and calculated radiances should occur at 0 and 100% cloud cover (i.e. clear-sky and opaque conditions). The cloud top pressure for semi-transparent or sub-pixel cloud is determined from the intersection of the linear fit to the observations and the curve through the calculated opaque radiances (see Schmetz *et al.* 1993, Fig. C1).

To summarize, the straight line through the clear-sky radiance pair $(R_{ir}^{clr}, R_{wv}^{clr})$ and the measured radiances (R_{ir}^{m}, R_{wv}^{m}) will pass through the point (R_{ir}^{o}, R_{wv}^{o}) on the curve through the calculated opaque radiances given by:

$$R^{o}_{wv} = R^{clr}_{wv} + \left\{ \frac{R^{clr}_{ir} - R^{o}_{ir}}{R^{clr}_{ir} - R^{m}_{ir}} \right\} (R^{m}_{wv} - R^{clr}_{wv}) \qquad (1)$$

The detailed application of the method involves choosing how to determine the linear relation between the measured radiances. Nieman *et al.* (1993) choose to use the line joining the average radiances of the warmest (clearest) and coldest (cloudiest) clusters of observations within the specified target area. Whyte (1997) suggests a linear regression using all the measured radiances and the calculated clear sky radiance pair within the chosen region.

Alternatively, the method can be applied pixel-by-pixel, in which case the pressure level at which the equation

$$\frac{R^{o}_{wv} - R^{clr}_{wv}}{R^{o}_{ir} - R^{clr}_{ir}} = \frac{R^{m}_{wv} - R^{clr}_{wv}}{R^{m}_{ir} - R^{clr}_{ir}} \qquad (2)$$

is more nearly satisfied is sought. This is the so-called 'Radiance ratioing method' (Menzel *et al.* 1983) applied to the IR and water vapour channels.

It should be noted that the method is, in fact, a correction for sub-pixel opaque cloud elements in conditions of varying cloud amount and not an explicit correction for semi-transparent cloud itself. Furthermore, the method assumes that the effective cloud emissivities in the IR and water vapour channels are equal, an approximation which cannot easily be justified.

3 Description of data

The satellite data are taken from the GOES imaging radiometer. The wavelength bands and resolution of the five channels are summarized in Table 3.1.

Channel	Wavelength (μm)	IGFOV (km × km)
1	0.52 - 0.72	1 × 1
2	3.78 - 4.03	4 × 4
3	6.47 - 7.02	8 × 8
4	10.2 - 11.2	4 × 4
5	11.5 - 12.5	4 × 4

Table 3.1: GOES-8 imaging channel characteristics.

The region studied extends roughly from 80-120°W and from 15-50°N, being chosen to comprise a variety of surface types and conditions. For data in the IR channels this region comprises 768 × 768 pixels. The region is subdivided into 'boxes' or 'subregions' of 32 × 32 pixels. All calculations are based on data within these subregions.

The radiative transfer calculations are performed for each subregion using a version of RTTOVS adapted to the GOES channels and analysed temperature and humidity profiles from both the ARPEGE and ECMWF models. The majority of the work presented here makes use of data at 12Z (GOES Slot 24), when profiles for both models are available. The profiles, which are originally on twenty atmospheric levels, are interpolated onto the forty levels required by RTTOVS.

4 Simulation of GOES radiances using NWP analyses

It is evident that the reliability of this technique depends critically on the accuracy of the simulated radiances, in particular those for clear sky conditions. This being so, it is useful to have some idea of the accuracy of the radiances calculated using the two model analysis profiles compared to those observed for clear scenes. Ideally, the observed clear scene radiance pair should lie on the theoretical curve joining the opaque cloud radiances. This is, however, seldom the case, the discrepancies arising due to the differences between the actual meteorological conditions (upper tropospheric humidity, surface temperature, etc) and those predicted by the NWP model. In an attempt to deal with this problem, Schmetz *et al.* (1993) require that the observed radiances be within 10% of the calculated IR-WV relationship. Nieman *et al.* (1993), on the other hand, apply a vertical shift to the calculated WV radiances to bring them into agreement with the observed values. (Note that this shifting of the calculated curve is only applied when the observed clear radiances lie above the computed values.)

In this section the differences between the clear sky radiances simulated using both ARPEGE and ECMWF analysis profiles are compared to those observed for clear scenes, these latter being identified using a cloud mask based on various threshold tests.

Infrared window radiances

Figure 4.1 shows scatter plots of the IR window radiance simulated using ARPEGE and ECMWF analyses against the observed GOES measurements for clear scenes. The data are for 12th, 23rd, 24th and 28th August 1998, all at 12Z, and are shown seperately for land and ocean regions. Each point represents the mean radiance of all the pixels identified as clear within each 32 × 32 subregion.

The two simulations show generally similar characteristics when compared to the observations, although the ECMWF calculations seem to demonstrate a systematic overestimate of the clear sky IR window radiance over land (Fig. 4.1c). This is seen more clearly in Fig. 4.2, which shows scatter plots of the differences between the calculated and observed radiances for the two simulations. Note that differences in both cases are of the order of 5% over the ocean and up to 10% over land.

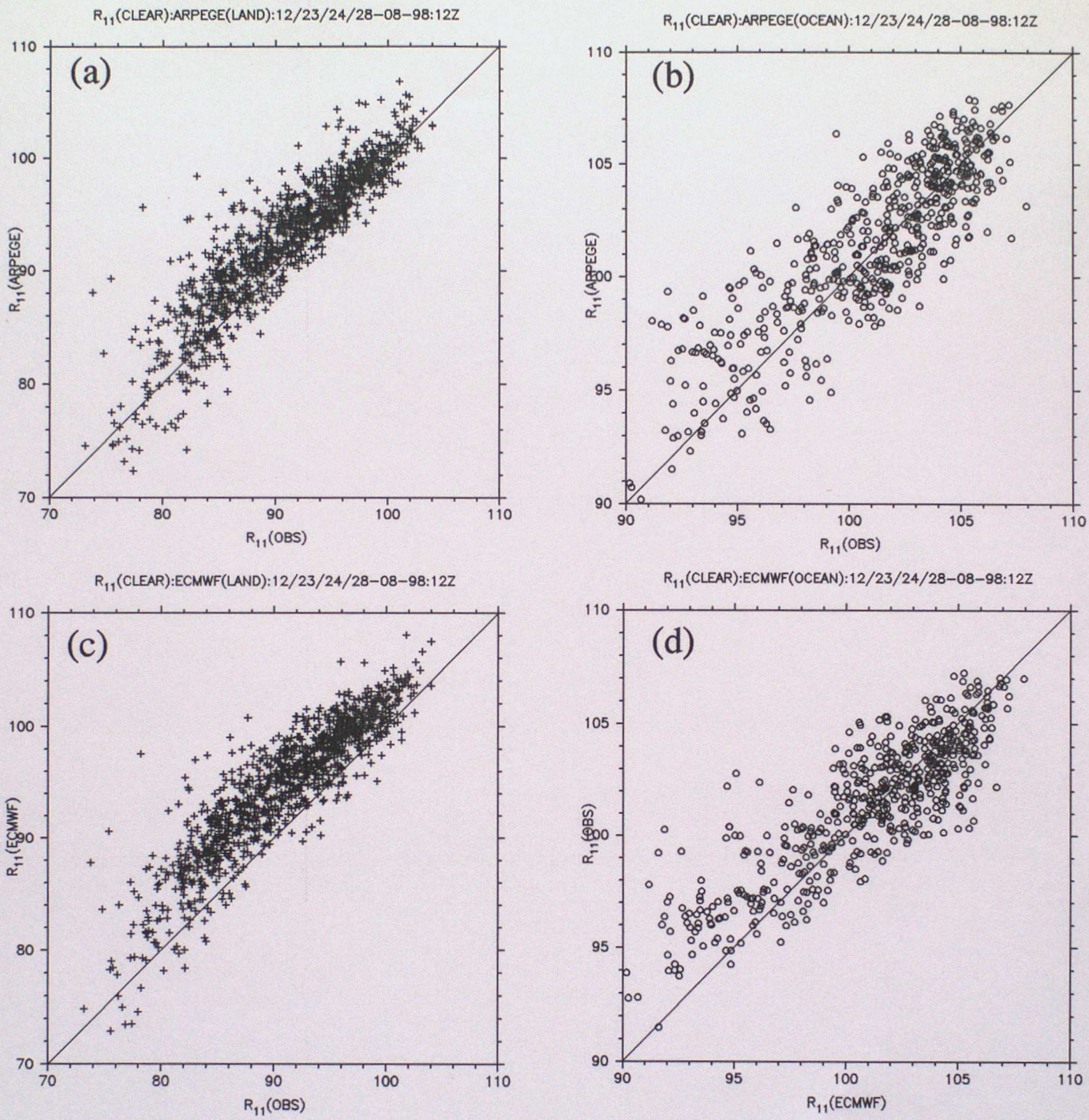

Figure 4.1: Scatter plots of the simulated versus observed clear sky IR window radiances: (a) ARPEGE over land; (b) ARPEGE over ocean; (c) ECMWF over land; (d) ECMWF over ocean. Data are for the 12th, 23rd, 24th and 28th August 1998 at 12Z. The line of perfect agreement is shown in each case. In this and all subsequent figures the radiance units are $mWm^{-2}\ sr^{-1}\ cm$.

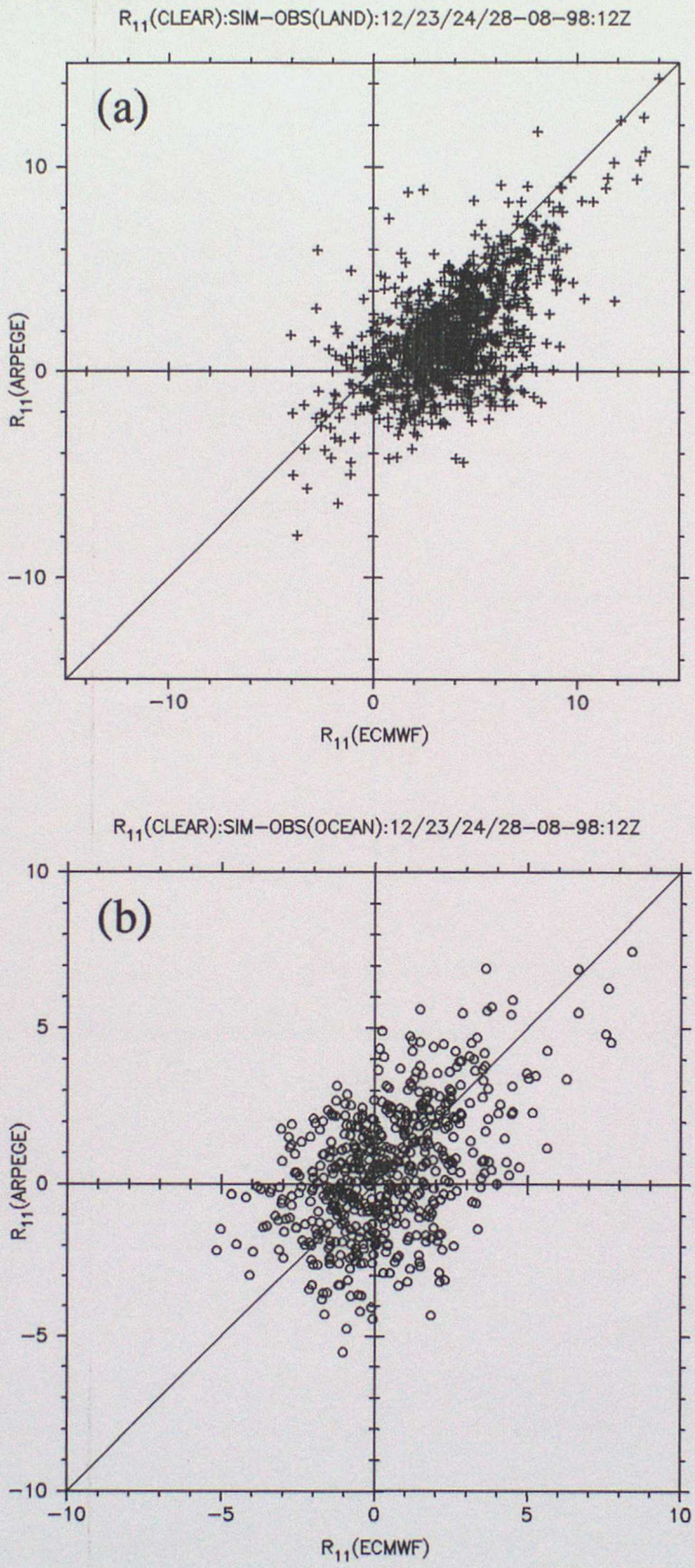

Figure 4.2: Scatter plots of the simulated minus observed IR clear sky radiances for the two simulations, using the data shown in Fig. 4.1: (a) Land; (b) Ocean.

Water vapour channel radiances

Figs. 4.3 and 4.4 show analagous plots to those shown in Figs 4.1 and 4.2 for the clear sky WV channel radiances. It is readily apparent that, compared to the IR window radiances, the simulated radiances differ much more from the observations and also from each other. Over land, the ARPEGE simulations appear to systematically underestimate the WV radiance while the ECMWF values show areas of both over- and underestimation, scattered approximately evenly about the line of perfect agreement. Over oceanic regions both simulations generally underestimate the clear sky WV radiance. The ECMWF values seem to be in slightly better agreement with the observations: note how the largest values are much better simulated for example. These findings are again highlighted by plottting the model differences against each other (Fig. 4.4).

Variations with time of day

As the ECMWF analyses are only available at 0 and 12Z, a local daytime comparison of the two simulated clear sky radiances is not possible. In order to consider the possibility of variations of the nature of the simulations with time of day Fig. 4.5 shows a comparison between ARPEGE IR and WV clear sky simulations for the 25th and 28th August 1998 at 18Z. The diurnal cycle of surface temperature leads to increased IR radiances at 18Z which are less well simulated than the lower values at 12Z (c.f. Figs. 4.5a and 4.1a). In fact there is clearly a tendency for the simulations to underestimate the observed values. The much weaker diural cycle of ocean temperature does not seem to systematically alter the simulation of the oceanic radiances (Figs. 4.5b, 4.1b).

Regarding the WV radiances, the systematic underestimation over both land and ocean is as much present at 18Z as at 12Z (c.f. Figs. 4.5c,d with Figs. 4.3c,d).

Summary statistics

As mentioned above, Schmetz *et al.* (1993) suggest that the calculated clear sky radiances must not deviate by more than 10% from the observed values in order to procede with this technique. Tables 4.1 and 4.2 show how application of this condition would affect the ARPEGE and ECMWF simulations for these particular dates. The data have (arbitrarily) been divided into three categories according to whether the magnitude of the discrepancy is <10%, 10-20% or >20% than the observed radiance.

Clearly, the application of the Schmetz *et al.* condition (or, indeed, any other similiar criteria) would potentially lead to the rejection of large numbers of pixels due primarily to discrepancies with the observed clear scene water vapour radiances.

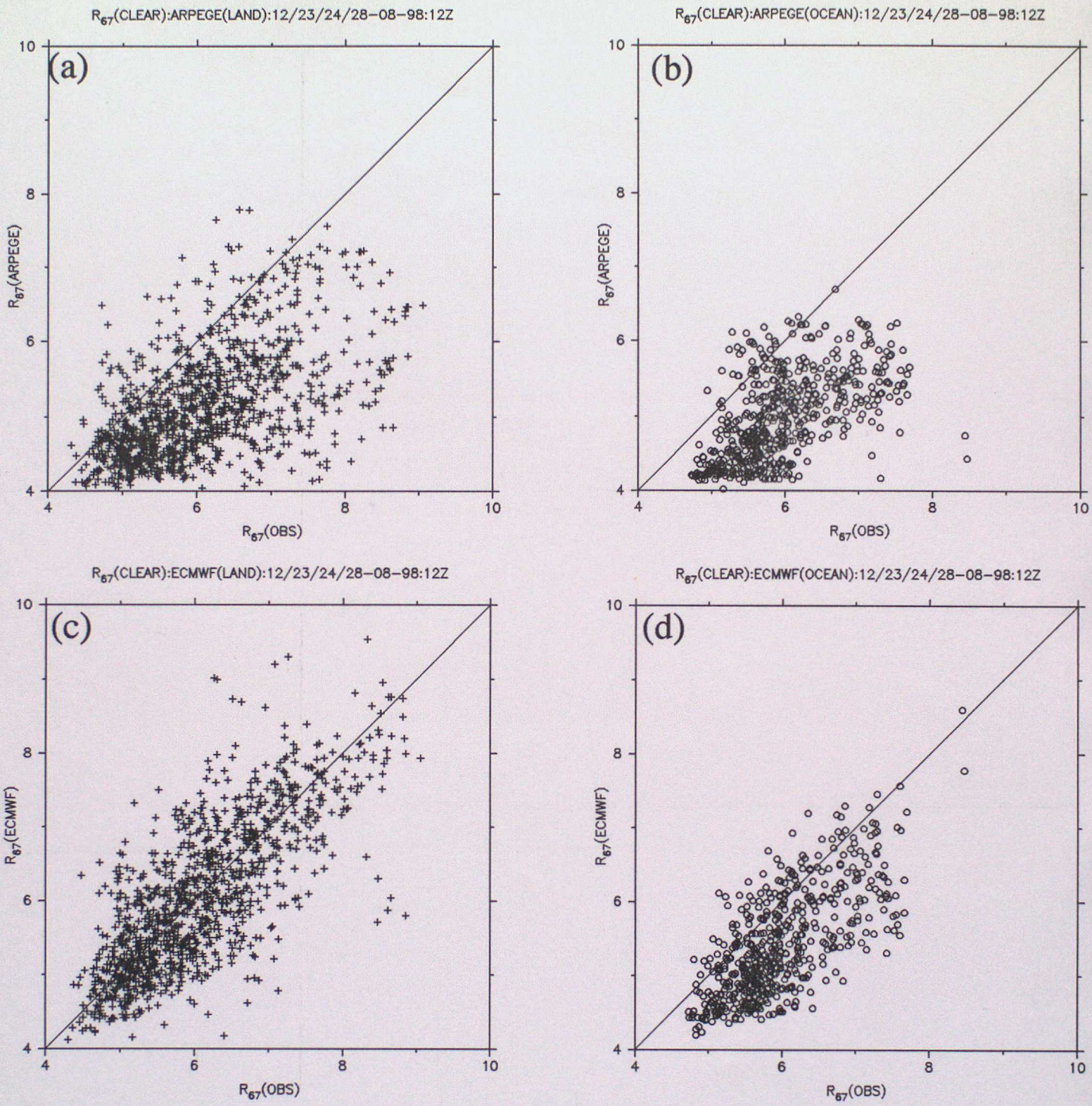

Figure 4.3: As Fig. 4.1 but for the simulated and observed clear-sky water vapour radiance.

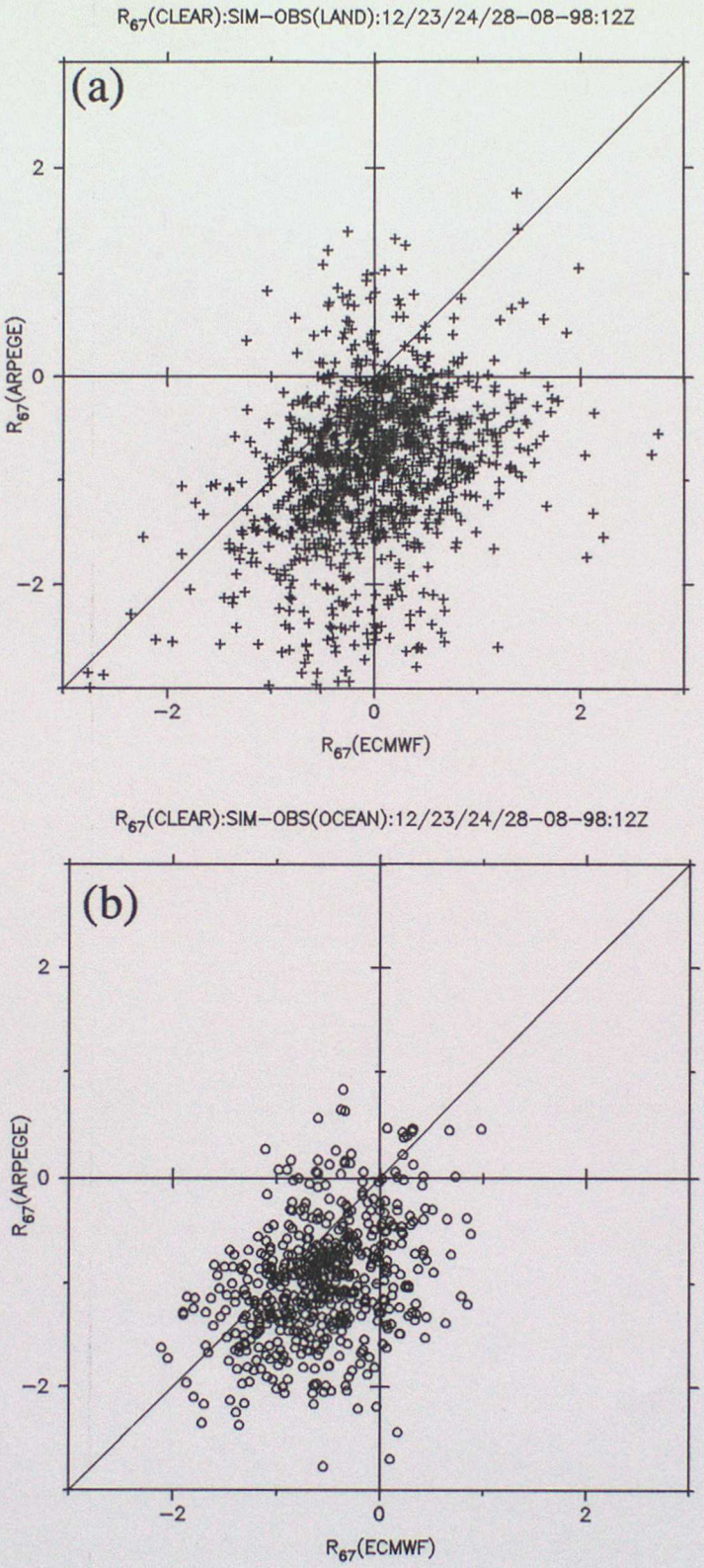

Figure 4.4: As Fig. 4.2 but for clear-sky water vapour radiances.

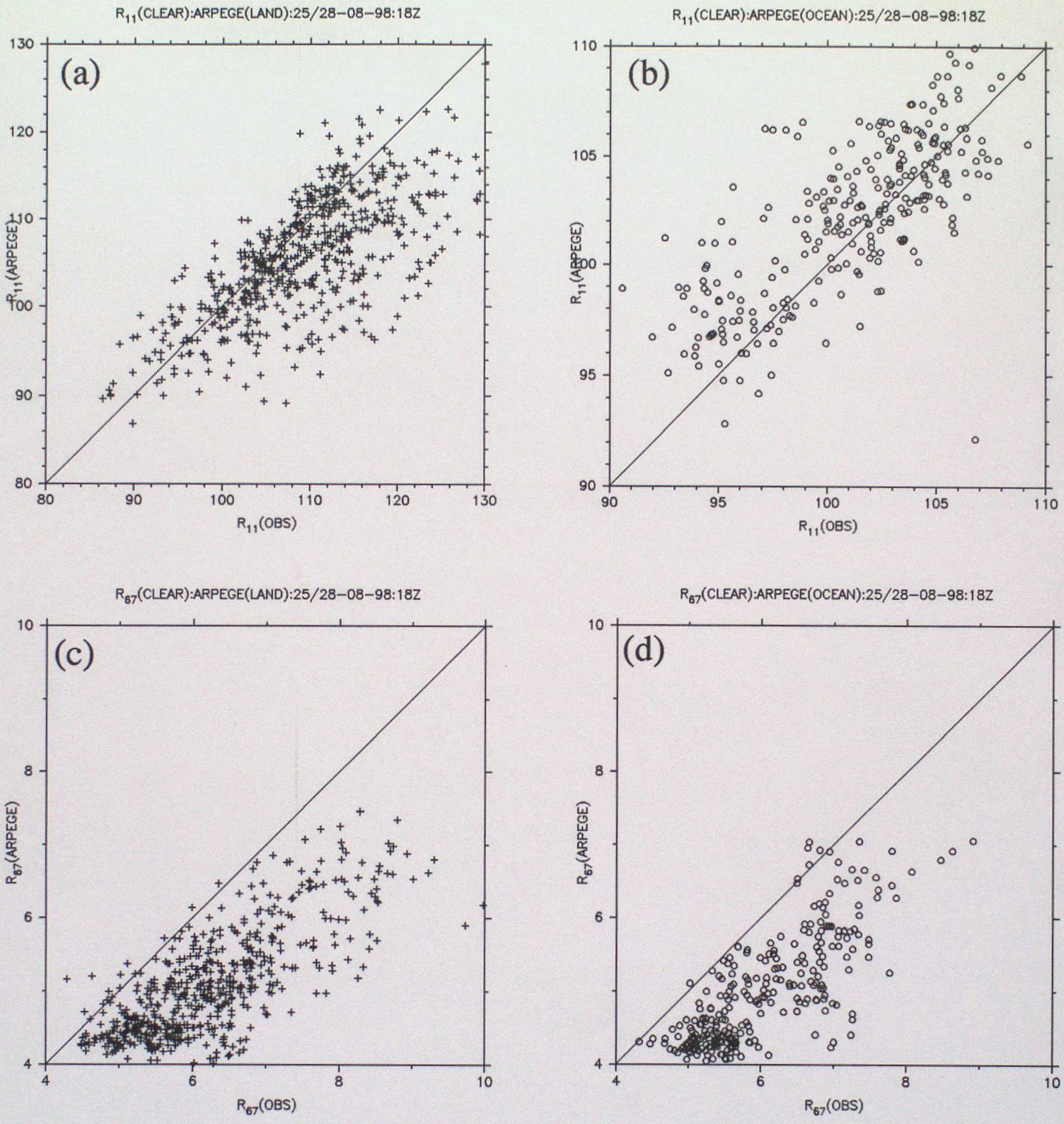

Figure 4.5: Scatter plots of ARPEGE and observed clear sky radiances for 25th and 28th August 1998 at 18Z: (a) IR land; (b) IR ocean; (c) WV land; (d) WV ocean.

IR WINDOW: LAND: 12Z

	No. of regions	< 10%	10 - 20%	> 20%
Arpege	1106	1087	18	1
Ecmwf	1106	1067	37	2

IR WINDOW: OCEAN: 12Z

	No. of regions	< 10%	10 - 20%	> 20%
Arpege	555	554	1	0
Ecmwf	555	554	1	0

Table 4.1a: Statistics for the IR window channel radiance differences shown in Fig. 4.2. The figures shown are the number of regions where the magnitude of the difference between the simulated and observed radiance is <10%, 10-20% or >20% of the observed value.

WV: LAND: 12Z

	No. of regions	< 10%	10 - 20%	> 20%
Arpege	1106	346	431	329
Ecmwf	1106	754	275	77

WV: OCEAN: 12Z

	No. of regions	< 10%	10 - 20%	> 20%
Arpege	555	111	261	183
Ecmwf	555	276	229	50

Table 4.1b: As above but for the WV channel differences shown in Fig. 4.4.

ARPEGE: LAND: 18Z

	No. of regions	< 10%	10 - 20%	> 20%
IRW	569	504	65	0
WV	569	107	228	234

ARPEGE: OCEAN: 18Z

	No. of regions	< 10%	10 - 20%	> 20%
IRW	279	274	5	0
WV	279	48	134	97

Table 4.2: As above but for the ARPEGE simulations only at 18Z shown in Fig. 4.5.

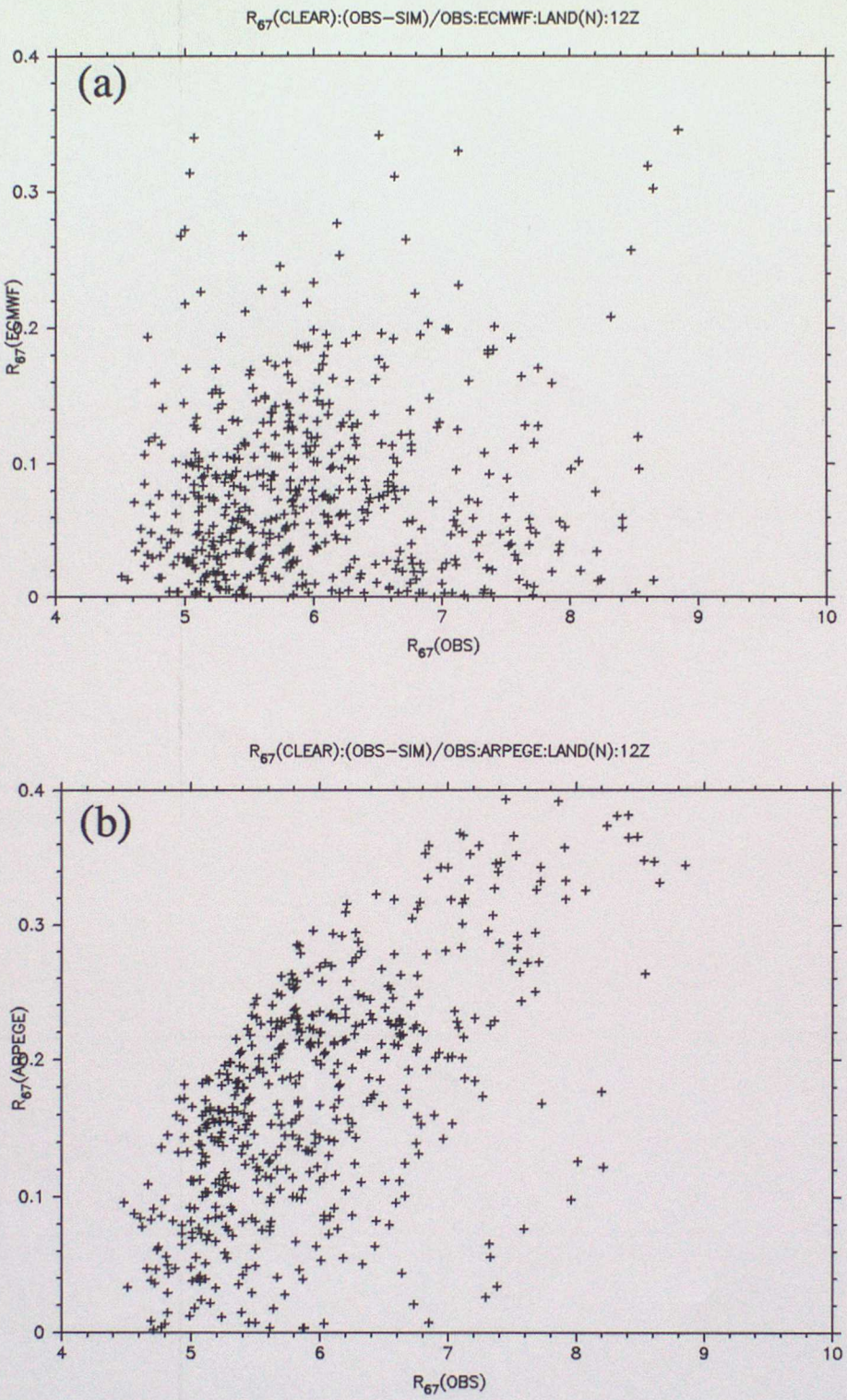

Figure 4.6: Magnitude of difference between the simulated and observed clear sky WV radiances versus the observed value for land segments in the northern half of the test region: (a) ECMWF; (b) ARPEGE.

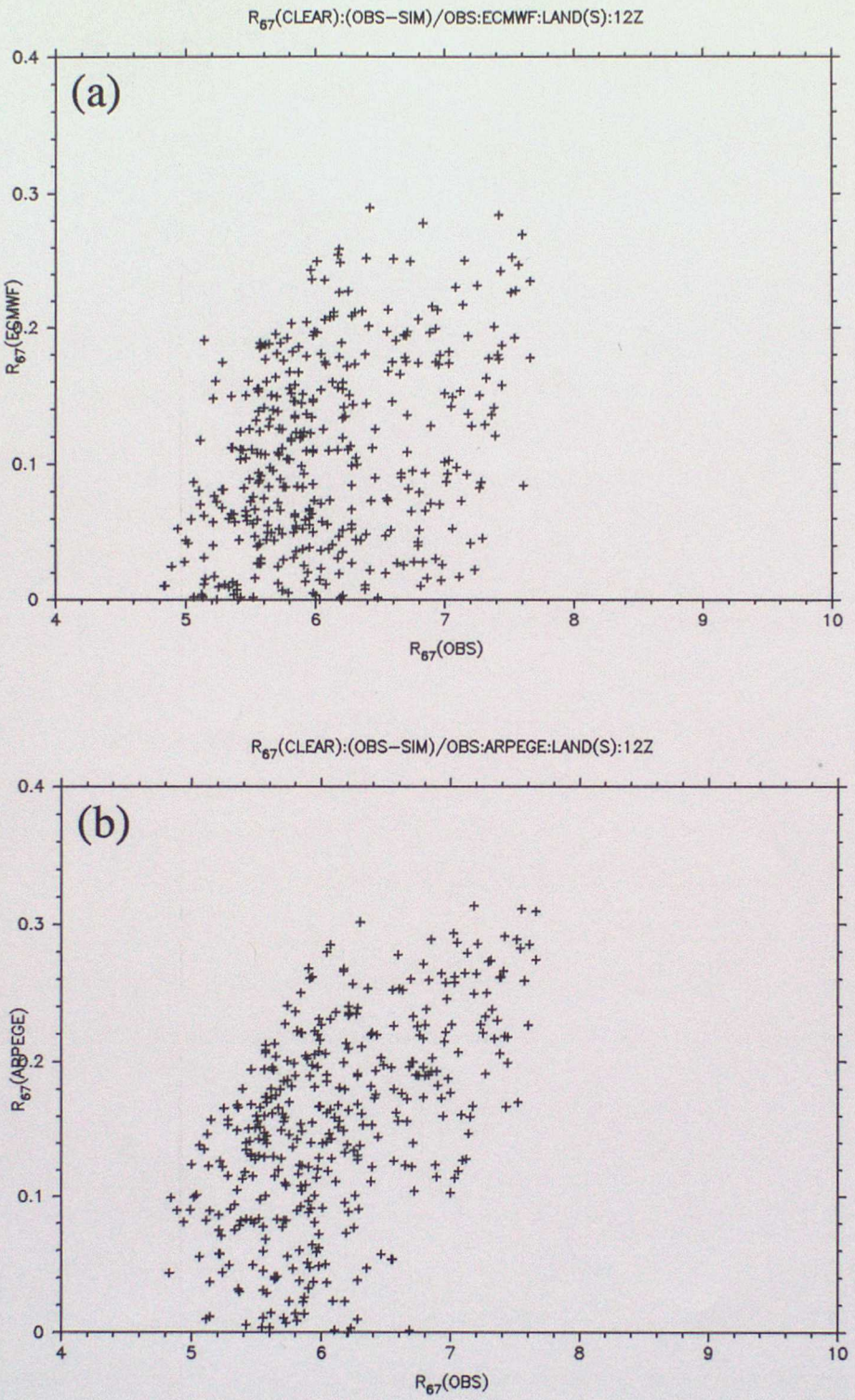

Figure 4.7: As Fig 4.6 but for the southern half of test region.

Geographical variations

Figure 4.6 shows scatter plots of the magnitude of the differences in the two simulations of the WV radiances divided by the observed values for land regions in the northern half of the test area. The ARPEGE simulations seem to show a systematic increase in this difference with increasing water vapour radiance, whereas no such clear trend is apparent in the ECMWF simulations.

In the southern half of the test region, however, both simulations show an increasing difference with increasing clear sky water vapour radiance (Fig. 4.7).

Discussion

Even though only a relatively small number of cases have been examined for one particular time of year, it is clear that a great deal of attention should be paid to the simulation of the clear sky radiances using any given NWP model profiles before proceeding with the application of the Eumetsat / Radiance Ratioing methods. This is of primary importance concerning the simulated water vapour radiances but may, in certain circumstances, also involve the IR window radiances.

Awareness of these discrepancies and their variation with surface type, latitude and time of day should help to clarify possible weaknesses in the cloud height detection technique and might suggest methods of accounting for the differences between the observed and simulated clear sky radiances.

These initial comparisons suggest that, at the present time, the ECMWF simulations are more reliable than those using the ARPEGE profiles, although the limited nature of this investigation means that this conclusion is by no means definitive.

5 Application of the water vapour - IR window intercept method

In this section the application of the method described in Section 2 to the GOES imager data is described and some examples of its use are presented.

Application of technique

The determination of the linear relation between the measured IR and water vapour radiances is, of course, of primary importance to the cloud height determination. Moreover, as shown in the previous section, differences between the model and observed (or, indeed, between models) clear sky water vapour radiances can have a large influence on this relation. This being so, three slightly different methods of inferring the linear relationship have been attempted:

(i) Clusters representing the hundred warmest (clear) and coldest (cloudy) (i.e. approximately 10%) of the IR radiances are identified. The mean IR and water vapour radiances for each cluster are calculated. Values lying outside of two standard deviations (in either channel) of the mean are rejected as outliers and the mean radiances, $(R_{ir}^{warm},R_{wv}^{warm})$ and $(R_{ir}^{cold},R_{wv}^{cold})$ are recalculated. The straight line joining these two radiance pairs defines the IR-water vapour relationship. This method resembles that employed by Nieman *et al.* (1993), although the clustering technique used here is considerably less sophisticated.

(ii) In this case the line is that joining the cold radiance pair of (a) and the clear sky radiance pair obtained from the model simulations.

(iii) Finally, use is made of the cloud mask to identify clear and cloudy pixels within the subregion. The mean IR and water vapour radiance of the hundred (or the total number if less than 100) warmest clear and coldest cloudy pixels is calculated and the line joining these two radiance pairs obtained. Note that (i) and (iii) should give approximately the same line if the region contains a mixture of clear and cloudy pixels.

For each case the intersection of the straight line with the calculated curve representing the opaque radiances is determined and the cloud top pressure level inferred. Height assignments either above the tropopause or below 500 hPa are rejected.

Example (a)

Figure 5.1 shows the GOES Channel 4 brightness temperature image for 12Z on 12th August 1998 for the test region together with the Channel 4 minus Channel 5 temperature difference image. From these two images areas of opaque and semi-transparent cloud can be identified. Note, for example, the two areas of opaque cloudiness in the bottom left of Fig. 5.1a which show very little contrast between the two channels. However, it is apparent that semi-transparent cloud lies between these two opaque centres. Also noticeable are areas of semi-transparent cloud in the bottom right and centre of Fig. 5.1b.

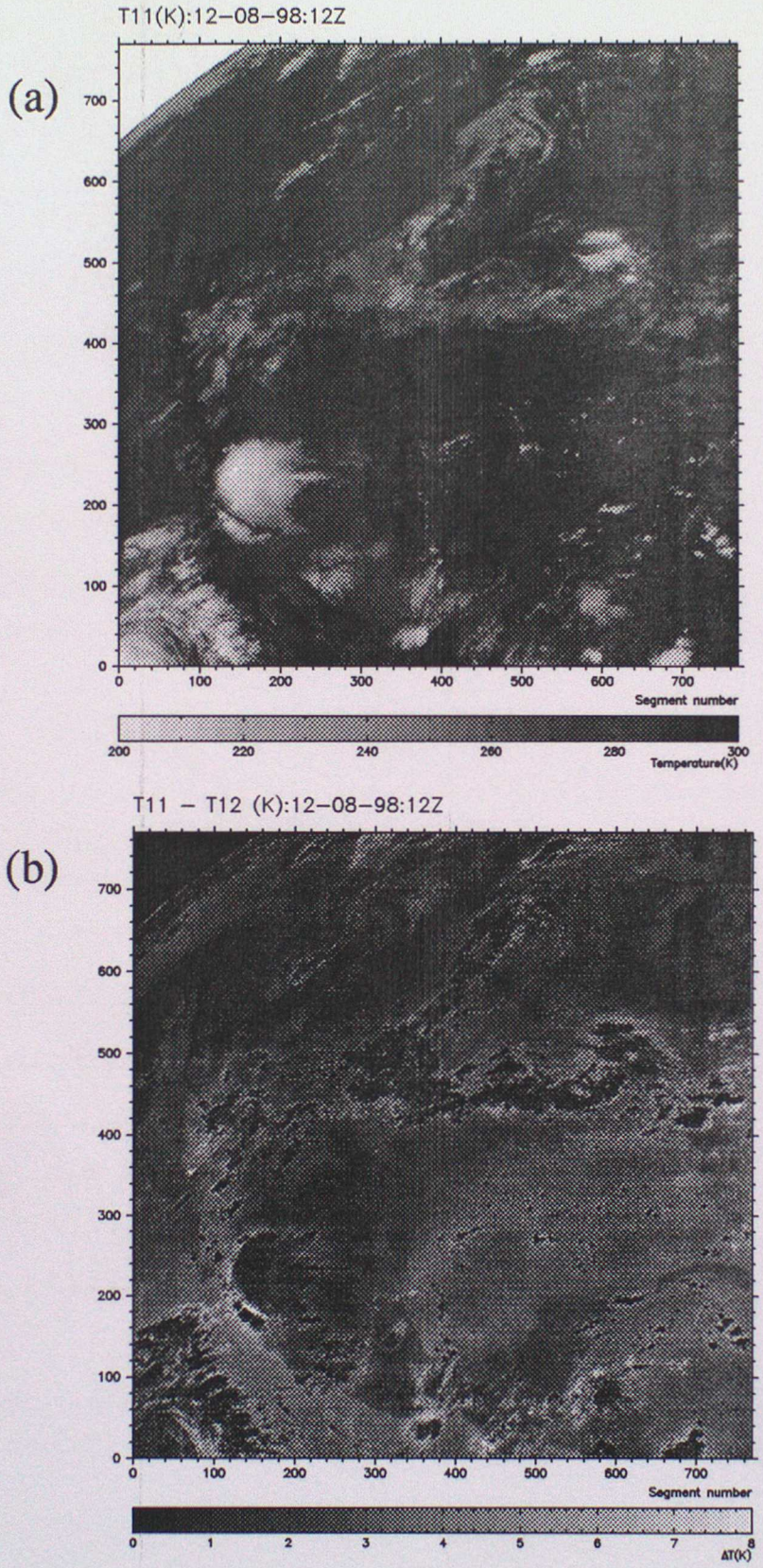

Figure 5.1: (a) GOES Channel 4 brightness tempererature and (b) Channel 4 minus Channel 5 brightness temperature difference for 12th August 1998 at 12Z.

Now, Figs. 5.2a-c show the cloud top pressure derived using methods (i), (ii) and (iii) described above and the ECMWF analysis profiles for this time slot. Fig. 5.2b shows method (ii) applied using the ARPEGE analyses. Inspection of these figures shows that, reassuringly, each method identifies the well-defined areas of opaque cloudiness in the original brightness temperature imagery. Consideration of the three methods using the ECMWF analysis profiles shows, moreover, that the areas of semi-transparent cloud identified in Fig 5.1b are also fairly well described. Comaprison of Figs. 5.2b and d suggests that the retrieval using the ARPEGE analyses is somewaht less successful. As might have been expected there isvery little difference between methods (i) and (iii) (Figs. 5.2a,c).

Example (b)

Figure 5.3 shows the Channel 4 and Channel 4 minus Channel 5 brightness temperature images for the 28th August 1998 also for 12Z. Regions of semi-transparent cloud are apparent in the bottom left of Fig. 5.3b which are barely discernable in the Channel 4 image. Fig. 5.4 shows the cloud top pressure retrieval using methods (ii) and (iii) together with the ECMWF analysis profiles. The well defined area of semi-transparent cloud in the bottom left of Fig. 5.3b seems to be well described in both cases. Other regions of semi-transparent cloud are also identified giving reason to believe that the application of this technique in these circumstances is at least qualitatively reliable.

Discussion

Although the method has been applied in a fairly simplified manner, the above examples demonstrate that the application of the water vapour-infrared window intercept technique to the GOES channels has at least the potential to furnish reliable estimates of the height of semi-transparent cloud. The availability of coincident split window IR channel measurements provides a source of useful validation data for the method by providing an alternative technique for identifying semi-transparent cloud. Clearly, many more examples need to be studied before any more concrete conclusions can be drawn.

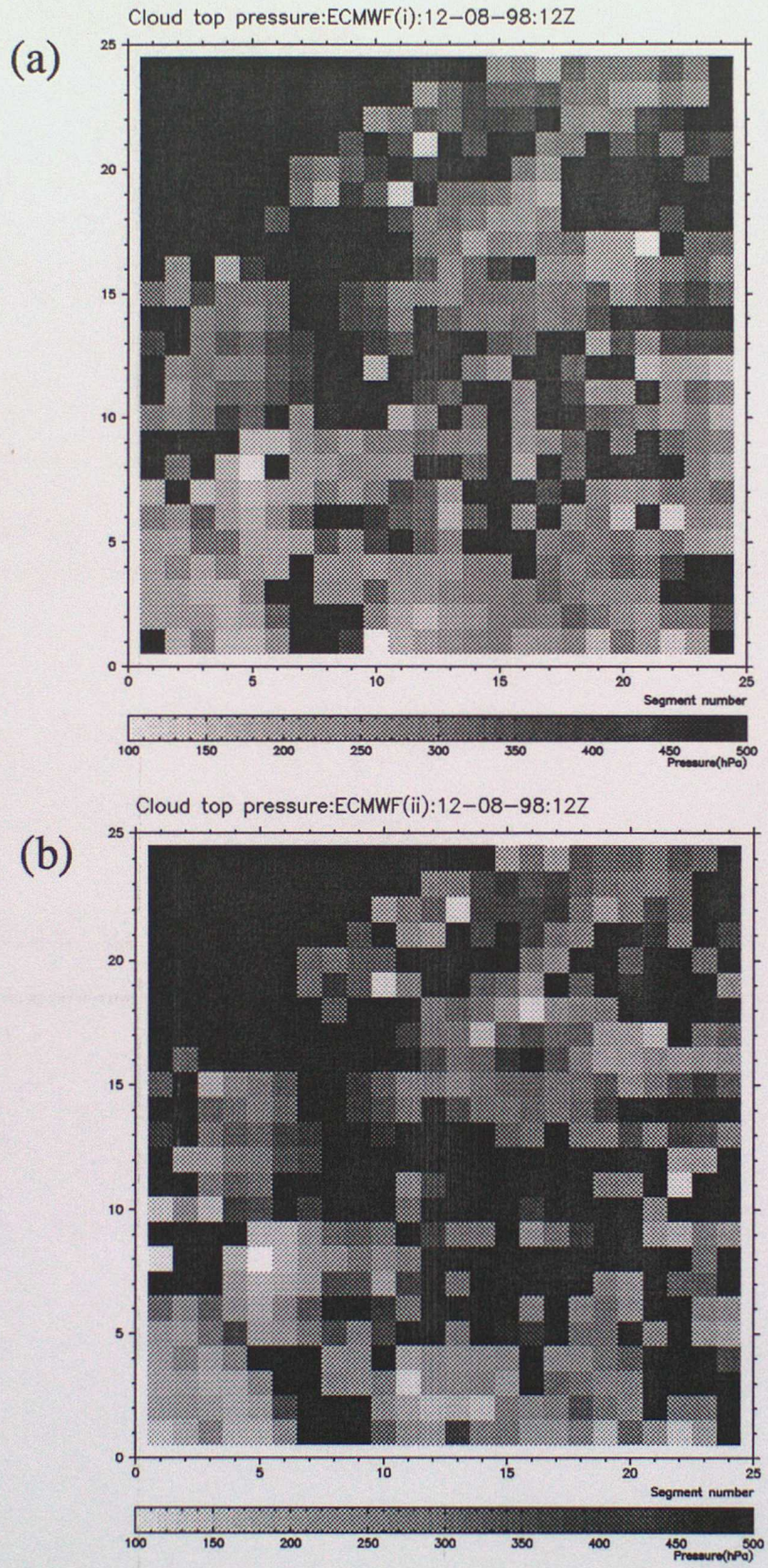

Figure 5.2: The cloud top height derived using methods (i), (ii) and (iii) and ECMWF profiles (a-c) and (d) method (ii) together with ARPEGE profiles.

(c)

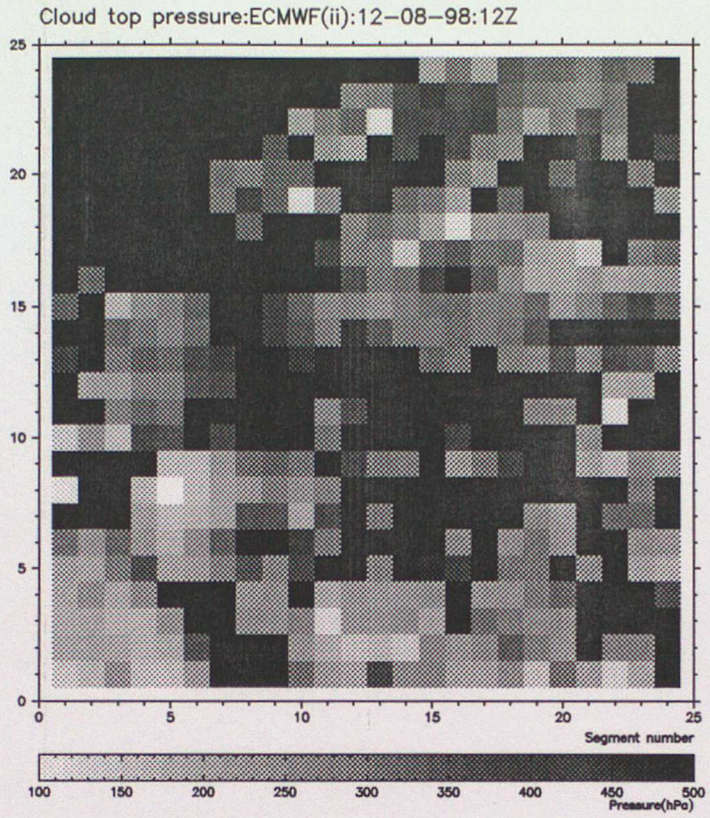

(d)

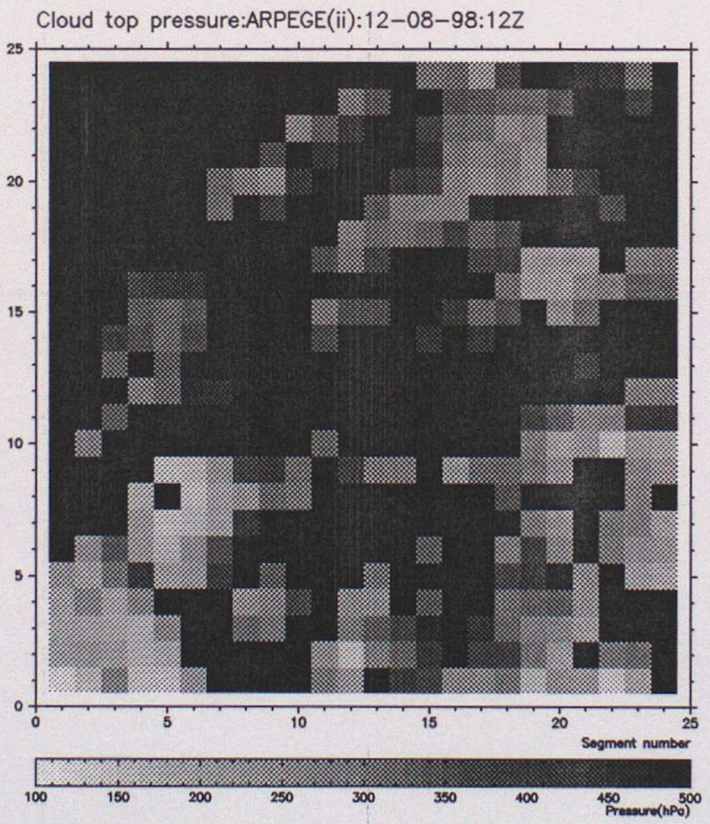

Figure 5.2: (Continued)

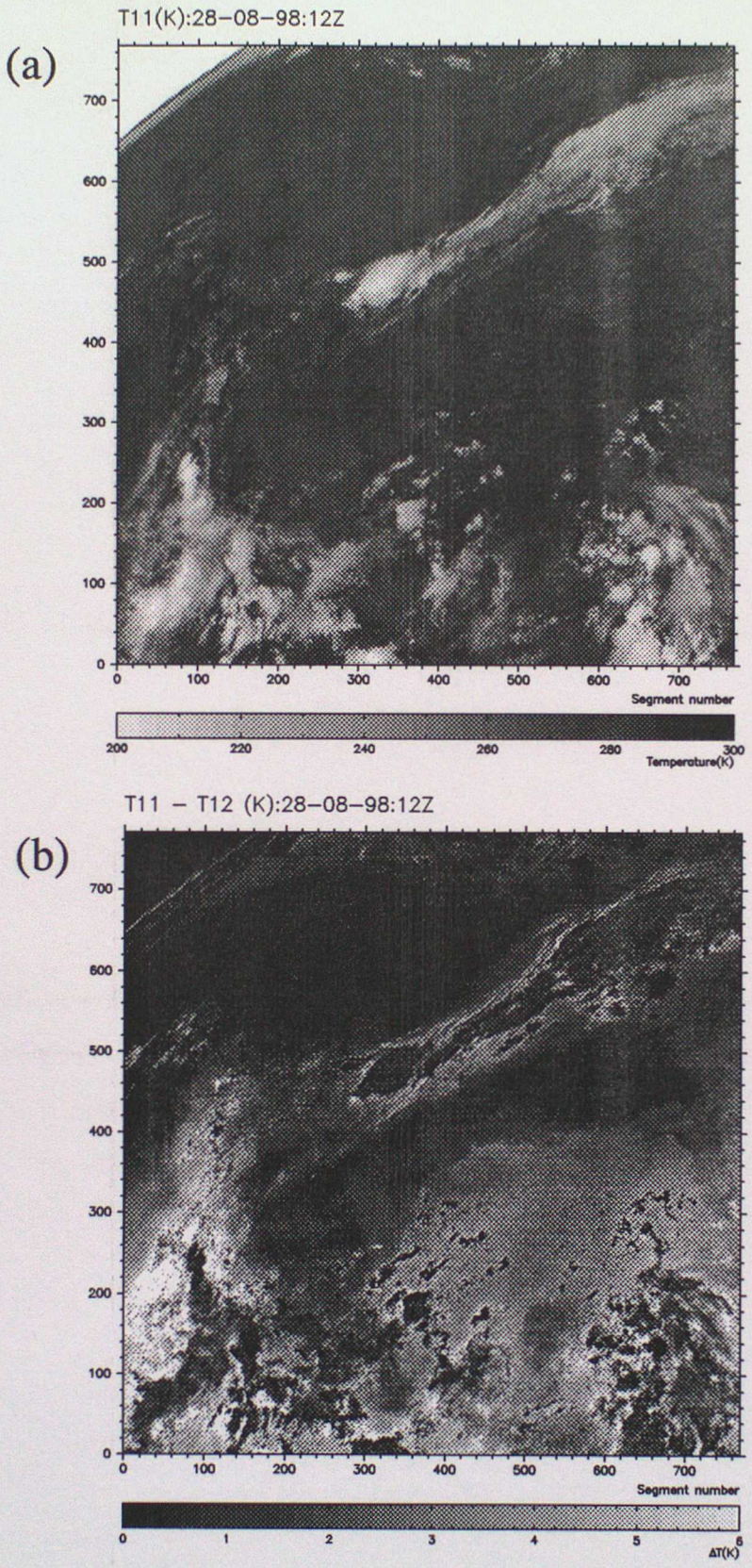

Figure 5.3: As Fig. 5.1 but for 28th August 1998 at 12Z

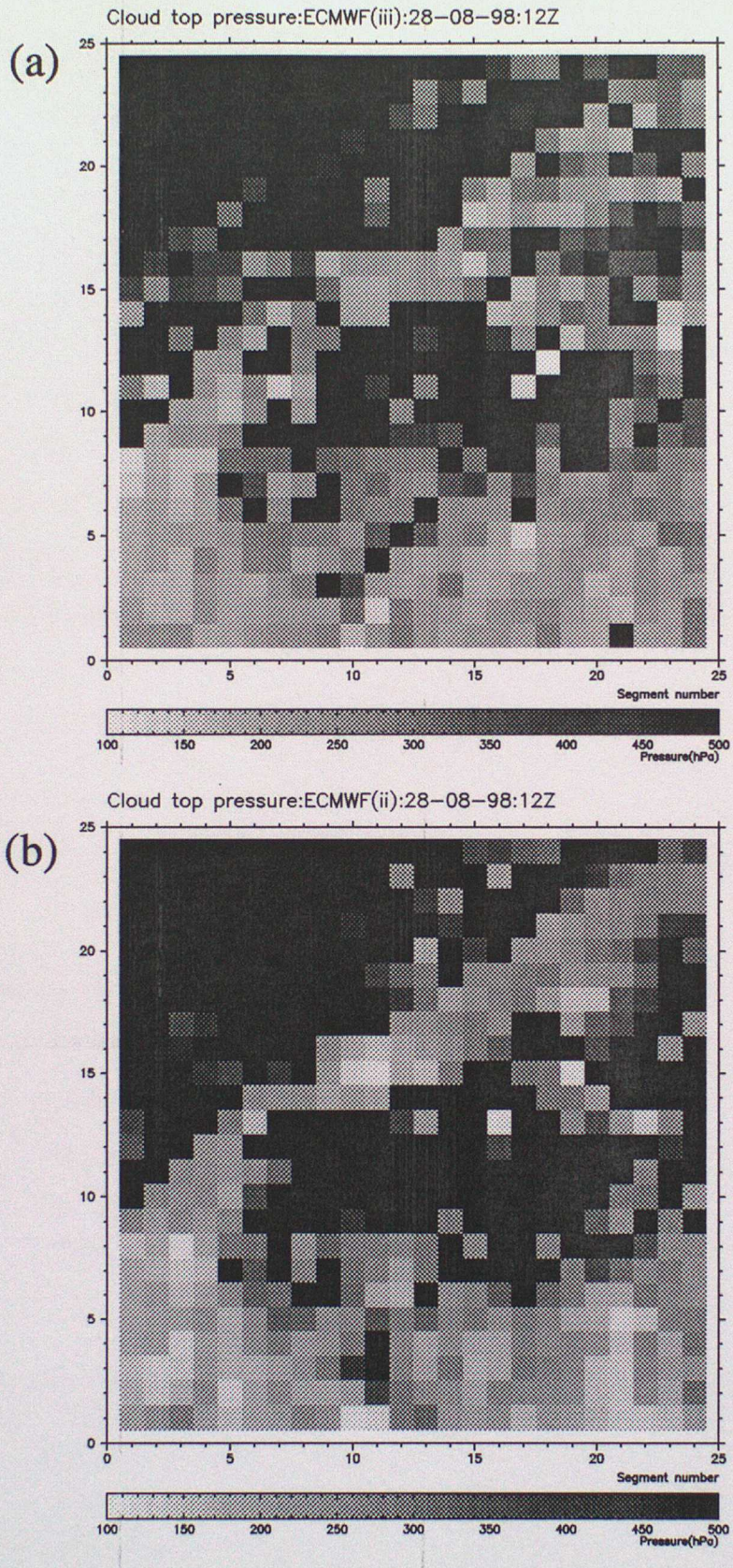

Figure 5.4: The retrieved cloud top pressure for 28th August 1998 at 12Z using methods (iii) and (i) and ECMWF analysis profiles.

6 Concluding remarks

This study represents an initial contribution to the application of the water vapour-infrared window technique to the GOES imager channels. The technique has been applied to GOES data and initial results show that, with refinements, potentially useful height estimates of semi-transparent cloud are possible.

As the application of this technique depends on the ability to correctly simulate clear sky radiances, an investigation of the clear scene radiances simulated using both ARPEGE and ECMWF analysis profiles was carried out. The main discrepancies between observed and simulated radiances occured in the water vapour channel. As the simulated opaque radiances using both analyses tend to be generally in good agreement, it is primarily the differences between the clear sky radiances which would lead to differing height estimates using this technique. The results of this study imply that use of the ECMWF analyses generally leads to simulated clear scene radiances in closer agreement with the observations. With an understanding of the nature of these differences, the possibility to apply some form of correction (based, for example on surface type or latitude) to the simulated radiances exists.

The method has been applied in a relatively straightforward manner with three slight variations. Clearly, other possibilities exist: for example, a linear regression could be performed using only those points classified as semi-transparent cloud using the IR split window measurents. The most useful next step would probably be to apply the method pixel by pixel (the radiance ratioing technique) and compare the cloud top pressures so retrieved to the present results. This could be done seperately for pixels classified *a priori* as opaque or semi-transparent cloud.■

References

Eyre, J.R. and W.P. Menzel, 1989: Retrieval of cloud parameters from satellite sounder data: A simulation study. *J. Appl. Meteor.*, **28,** 267-275.

Inoue, T., 1985: On the temperature and effective emmisivity determination of semi-transparent cirrus cloud by bi-spectral measurements in the 10 μm window region. *J.Meteor. Soc. Jpn.*, **63,** 88-99.

Lin, X. and J.A. Coakley, 1993: Retrieval of properties of semitransparent clouds from multispectral infrared imagery data. *J. Geophys. Res.*, **98,** 18 501- 18514.

Nieman, S.J., J. Schmetz and W.P. Menzel, 1993: A comparison of several techniques to assign heights to cloud tracers. *J. Appl. Meteor.*, **32,** 1559-1568.

Menzel, W.P., W.L. Smith and T.R. Stewart, 1983: Improved cloud motion wind vector and altitude assignment using VAS, *J. Clim. Appl. Meteor.*, **22,** 377-384.

Schmetz, J., K. Holmund, J. Hoffman, B. Strauss, B. Mason, V. Gaertner, A. Koch and L. Van De Berg, 1993: Operational cloud-motion winds from meteosat infrared images. *J. Appl. Meteor.*, **32,** 1206-1225.

Szejwach, G., 1982: Determination of semi-transparent cirrus cloud temperature from infrared radiances: Application to Meteosat., *J. Appl. Meteor.*, **21,** 384-393.

Whyte, K.W., 1997: A method for the treatment of semi-transparent cirrus in the Nimrod cloud-top height scheme and its effect on the mesoscale model. *F.R. Div. Tech. Rep. No. 219.* (U.K. Met. Office, Bracknell, U.K.)